Estuaries and Coasts (2013) 36:300–318
DOI 10.1007/s12237-012-9574-z

Suspended-Sediment Flux and Retention in a Backwater Tidal Slough Complex near the Landward Boundary of an Estuary

Tara L. Morgan-King · David H. Schoellhamer

Received: 5 April 2012 / Revised: 30 October 2012 / Accepted: 4 November 2012 / Published online: 30 November 2012

Abstract Backwater tidal sloughs are commonly found at the landward boundary of estuaries. The Cache Slough complex is a backwater tidal region within the Upper Sacramento–San Joaquin Delta that includes two features that are relevant for resource managers: (1) relatively high abundance of the endangered fish, delta smelt (*Hypomesus transpacificus*), which prefers turbid water and (2) a recently flooded shallow island, Liberty Island, that is a prototype for habitat restoration. We characterized the turbidity around Liberty Island by measuring suspended-sediment flux at four locations from July 2008 through December 2010. An estuarine turbidity maximum in the backwater Cache Slough complex is created by tidal asymmetry, a limited tidal excursion, and wind-wave resuspension. During the study, there was a net export of sediment, though sediment accumulates within the region from landward tidal transport during the dry season. Sediment is continually resuspended by both wind waves and flood tide currents. The suspended-sediment mass oscillates within the region until winter freshwater flow pulses flush it seaward. The hydrodynamic characteristics within the backwater region such as low freshwater flow during the dry season, flood tide dominance, and a limited tidal excursion favor sediment retention.

Keywords Suspended sediment · Sediment transport · Turbidity · Sediment retention · Tidal asymmetry · Tidal slough

Introduction

Background

Sediment is an integral component of a healthy functioning estuarine habitat. In California's Sacramento–San Joaquin River Delta, turbidity is a key driver for pelagic fish habitat (Feyrer et al. 2007). For example, water clarity and endangered delta smelt (*H. transpacificus*) occurrence is inversely related (Feyrer et al. 2011; Nobriga et al. 2008). Delta smelt require turbid water for feeding success in their larval life stage (Baskerville-Bridges et al. 2004), to avoid predation (Feyrer et al. 2007), and as a migratory cue (Sommer et al. 2011). Declining turbidity within the estuary (Jassby et al. 2002, Schoellhamer 2011) is one of several factors that may explain a severe decline in the abundance of delta smelt and other fish species in the 2000s, known as the pelagic organism decline (Sommer et al. 2007).

Tidal marsh plays an important ecological role and provides habitat for pelagic fish (Moyle et al. 1986; Brown 2003; Nobriga et al. 2005), yet 95 % of the historical marsh has been removed from the estuary (Atwater et al. 1979). Throughout the Delta, tidal marshes were artificially diked in the late 1800s and early 1900s to create islands used for agriculture. Since the late nineteenth century, the Delta has been converted from a seasonally brackish marsh to an area with hydraulically isolated islands that are >5 m below mean sea level (Reed 2002) and are surrounded by a network of leveed channels of increasing water clarity (Nobriga et al. 2005). Presently, resource managers are planning and implementing tidal marsh restoration projects intended to restore ecological function to the Delta (Kneib et al. 2008; Delta Stewardship 2011). The functioning of tidal freshwater marsh is not well understood, but sediment supply, transport, and resuspension mechanisms are critical components to the investigation of both aquatic habitat stability and restoration potential because sediment is essential for the creation and sustainability of habitats such as tidal marsh.

This study focuses on a landward estuarine region within the upper Delta, known as the Cache Slough complex. This turbid backwater area includes dead end channels and surrounds a shallow freshwater flooded island, Liberty Island,

T. L. Morgan-King (✉) · D. H. Schoellhamer
US Geological Survey, Placer Hall 6000J. St,
95819, Sacramento, CA, USA
e-mail: tamorgan@usgs.gov

which serves as a prototype for restoration because tidal flooding was restored to the former agricultural island in 1998 when storm induced levee failures were not repaired. Liberty Island is now primarily open water with fringe marsh habitat. The Cache Slough complex is not well understood but is likely reminiscent of a predeveloped Delta habitat (Grossinger and Whipple 2009; Whipple 2010). Although turbidity throughout the central and western Delta has been decreasing over multiple decades, the complex has been recognized as a more turbid location favoring endangered delta smelt (Nobriga et al. 2005) where they are utilizing the near-shore habitats of the complex on a year round basis (Sommer et al. 2009, 2011). It is important to understand the mechanisms that drive this turbid and functional slough complex both for water and resource managers. The results from this study can be useful to both science and management throughout the Delta estuary and other regions. Additional features of the region that may be attractive to native fish include large amounts of shallow water habitat and high prey densities (Lehman et al. 2010).

We observed hydrodynamic characteristics and sediment transport processes around the area including freshwater inflow, seaward outflow, and deposition from July 2008 through 2010 to determine the physical mechanisms that account for the relatively high turbidity in this area. Specifically, we address two questions: (1) Does Liberty Island play a dominant role on the hydrodynamics and sediment concentrations of the Cache Slough complex? and (2) Is the turbidity within the Cache Slough complex dependent on localized production from wind-wave and tidal resuspension coupled with subsequent local tidal oscillation? Addressing these questions will provide greater insight into the functioning of tidal freshwater habitats, which may help guide their restoration.

There have been many studies describing the mechanisms of sediment transport within estuaries, and it is well established that tidal currents, gravitational circulation, and wind can create areas of elevated suspended-sediment concentration. Sediment export is often related to large freshwater flow episodes, though researchers have also observed landward transport and sediment trapping during low flows (Guezennec et al. 1999; Geyer et al. 2001; Kitheka et al. 2002; Uncles et al. 2006). Landward residual transport within an estuary is most commonly related to gravitational circulation, but tidal processes can be equivalent to sediment trapping due to gravitational circulation (Sommerfield and Wong 2011; Allen et al. 1980; Uncles et al. 1985). Other researchers have found estuarine turbidity zones enhanced by the oscillation of an isolated suspended-sediment mass (Ganju et al. 2004; Uncles and Stephens 1993; Grabemann and Krause 1994; Grabemann et al. 1997). Furthermore, the direction of sediment flux can be time dependent and spatially variable.

Few studies though have been published on sediment transport in tidal backwater and dead-end channels. Kitheka et al. (2002, 2005) found sediment trapping due to flood dominant currents in the backwater zone of Mwache Creek, Kenya. (Ganju et al. 2004) observed sediment masses that tidally oscillated between San Francisco Bay and tributary creeks with negligible freshwater flow. Tidal excursion and slack tide deposition limited the range of the sediment masses. The purpose of this paper is to describe the sediment flux and mechanisms for turbidity maintenance in the backwater zone where there is absence of density circulation.

Sacramento–San Joaquin Delta

The Sacramento–San Joaquin Delta is within the San Francisco Estuary, the largest estuary on the west coast of the USA (Fig. 1). It drains the freshwaters from California's two largest rivers, the Sacramento and San Joaquin, respectively, as well as their tributaries. The estuary transitions from a highly saline 30 PSU and tidal dominated environment within the San Francisco Bay to the tidal but freshwater <1 PSU dominated Sacramento–San Joaquin Delta. The estuary experiences mixed semi-diurnal tides and the position of the saltwater interface (2 PSU) is typically in the Western Delta or Suisun Bay. Approximately 80 % of the freshwater flow and sediment (roughly 1,000 kt annually) into the Delta comes from the Sacramento River. The Delta provides drinking water to some 25 million Californians (Mac Nally et al. 2010), and freshwater diversions have altered the tidal patterns and hydrodynamics of the Delta (Kimmerer 2002; Nobriga et al. 2005).

The primary source of sediment into the Delta is the Sacramento River (including the Yolo Bypass) providing approximately 85 % of the total supply (Wright and Schoellhamer 2005). Suspended load accounts for 87–99 % of the total load and is predominantly fine sediment less than 63 μm in diameter (Schoellhamer et al. 2012). Much of the sediment is transported during the winter when the onset of seasonal rain initiates a "first flush" of freshwater downstream carrying a large pulse of sediment. Watershed sediment supply has been severely altered since the late 1800s hydraulic mining era when a large amount of sediment washed into Central Valley rivers and the Bay (Gilbert 1917. Sediment concentrations in the Sacramento River have gradually declined by about 50 % since 1957 (Wright and Schoellhamer 2004). Concurrent with this decline, total suspended solids within the Delta also decreased by approximately one half from 1975–1995 (Jassby et al. 2002). Major factors for the decline include reduction of supply from hydraulic mining within the watershed (James 2004), flow attenuation, and reservoir trapping (Arthur and Ball 1979; Wright and Schoellhamer 2004), trapping in flood bypasses

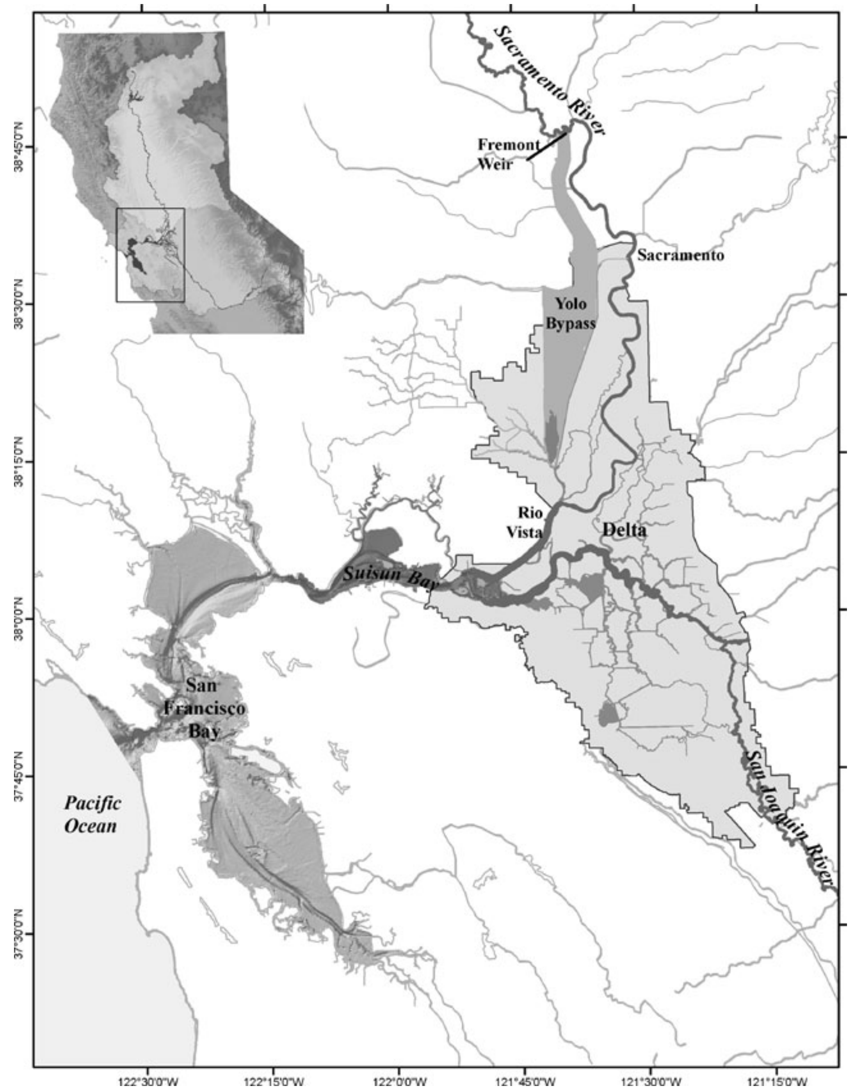

Fig. 1 The San Francisco Bay–Delta Estuary within Northern California. The *inset* shows the extent of the Sacramento and San Joaquin Watersheds as they merge forming the Estuary. The Sacramento–San Joaquin Delta (east of Suisun Bay) is shown as the *light gray polygon*

and diversions (Singer et al. 2008), levee construction and river bank protection in the Sacramento River (USFWS 2000) and trapping within expanding beds of non-native aquatic weeds within the Delta (Jassby and Cloern 2000; Champion and Tanner 2000; Wilcox et al. 1999). Tidal currents and wind waves throughout the Delta can resuspend the predominantly fine bottom sediments (Schoellhamer et al. 2012).

Study Area Description

The Cache Slough complex and specifically Liberty Island are at the southern most extent of the Yolo Bypass, the primary floodplain of the Lower Sacramento River (Sommer et al. 2008), where numerous lands and waterways join (Fig. 2). The Yolo Bypass diverts water from the Sacramento River, primarily at the Fremont Weir around the Sacramento metropolis, during large flow pulses induced by precipitation runoff and snowmelt predominantly in the winter and early spring. At southernmost extent of the Bypass, Liberty Island (a former leveled agricultural tract) is extremely shallow even upon high tide (ranging from intertidal at the extreme north to generally 1–2 m deep). Miner Slough (maximum depth of 6 m) is tidal yet highly influenced by the Sacramento River; its mouth meets Cache Slough below the Sacramento River Deep Water Ship Channel, which is a dead-end channel at the Port of Sacramento. One third of the width of the ship channel is dredged approximately 11 m deep with two thirds of the channel consisting of shallow shoals along the banks. Cache Slough above Liberty Island is a low flow channel with maximum depth of about 6.3 m and contains multiple shallow shoals. Cache Slough runoff primarily comes from Ulatis Creek to the west, which drains a large watershed from the Coast Range, the City of Vacaville, and numerous agricultural lands (roughly 4,500 km^2). The water within Miner Slough, comparatively, is from the Sacramento River. The Sacramento River watershed drains from a more

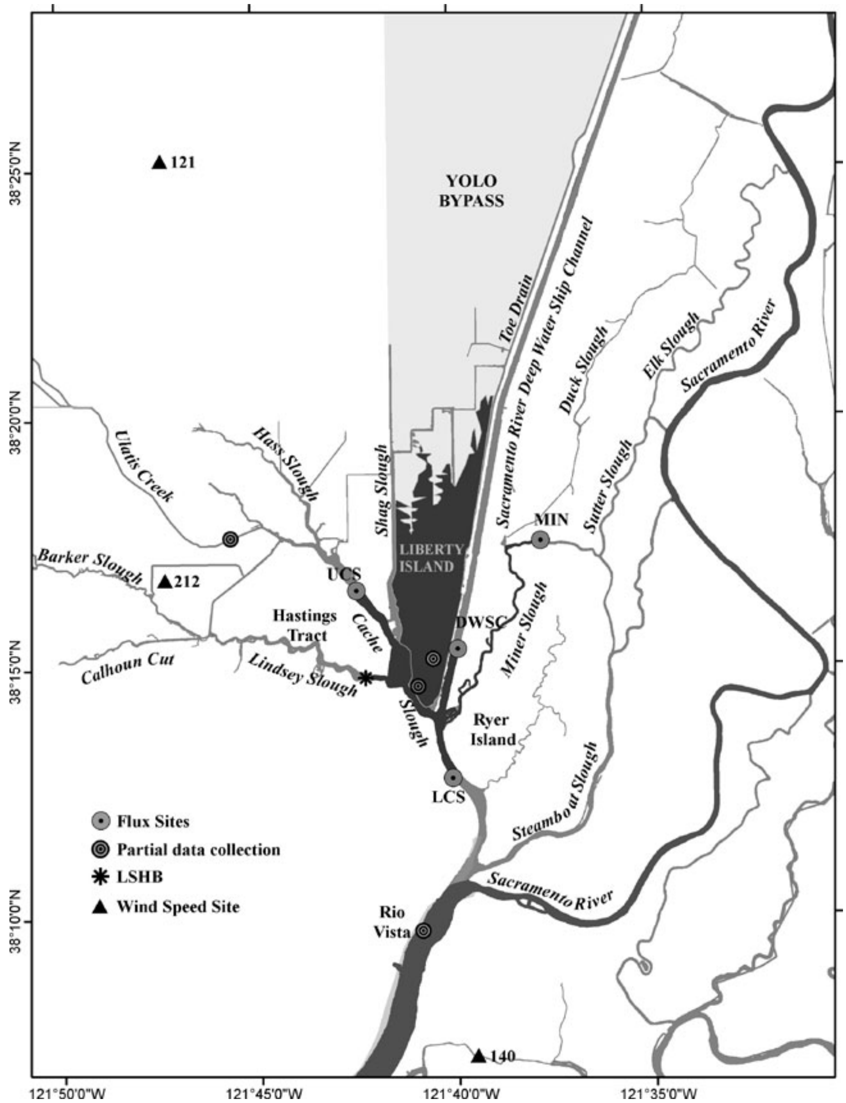

Fig. 2 The location of the Cache Slough complex in the Northern Sacramento–San Joaquin Delta surrounding the flooded Liberty Island and data collection sites. The flooded portion of Liberty Island and the control volume is shown as the *dark gray area* within the site boundaries

extensive landscape (nearly 70,000 km^2) of Northern California. Additional west side tributaries to Cache Slough include Hass, Shag, and Lindsey Slough. All these waterways come together into Cache Slough, which downstream from the mouth of Miner Slough is approximately 18 m deep before it merges with the mainstem Sacramento River near Rio Vista. Water pumps are located approximately 10.5 km upstream from the Cache–Lindsey confluence on Barker Slough, a tributary of Lindsey Slough.

Methods

Continuous Monitoring Data Collection Methods

We installed instrumentation at four sites within the Cache Slough complex beginning in July 2008 (Fig. 2) to measure the suspended-sediment flux (SSF) into and out of the region. This paper focuses on the measurements from July 2008 through December 2010. The four sites include Miner Slough at the Highway 84 Bridge (MIN) (USGS station number 11455165, http://waterdata.usgs.gov/ca/nwis/) Sacramento Deep Water Shipping Channel at Channel Marker 53 (DWSC) station 11455335, Upper Cache Slough (UCS) station 11455280, and Lower Cache Slough (LCS) at station 11455350. Sites UCS and MIN were used to measure wet season sedimentation rates into the complex. The locations of the four stations were intended to allow analysis of tidal resuspension dynamics during the dry season when delta winds influence the region. We expected sediment resuspension from shallow shoals and wanted to understand the characteristics of the dead end channels (DWSC and UCS). Continuous measurements at all locations consisted of conductivity, temperature, depth, and optical (nephelometric) sensor multiprobes (CTDO). The multiparameter instruments are all located 1.2 m above the bed, except for DWSC (0.6 m) due to the shallow location at the channel marker installation. These sites were also equipped with acoustic Doppler velocity meters (ADVMs). All sites are side lookers, except at UCS where the instrument is upward looking. The instrument logging interval for all parameters was 15 min; positioning, frequency, sampling, and averaging intervals are shown in Table 1. Additionally, we collected data during the latter part of 2010 at the main Liberty Island breach (turbidity beginning August 2010 and velocity beginning December 2010) and within the interior (turbidity beginning July 2010) to better understand the directional sediment flux at the main south breach and wind–wave resuspension within the island.

Water Velocity and Discharge

The California Department of Water Resources and other USGS personnel calculated channel discharge from the ADVM data using the index velocity method (Ruhl and M.R. Simpson 2005). In brief, the index velocity is compared to a channel-average velocity measured along a transect during approximately monthly site visits using a moving boat equipped with an acoustic Doppler current profiler (ADCP). A rating curve is created from this comparison and a 15-min time series of channel-average velocity is generated. Regression statistics for the rating curves are given in Table 1. Cross-sectional area is extracted from the ADCP geometry data, and a continuous stage–area relationship is calculated. Cross-sectional discharge (Q_{xs}) is calculated from the product of cross-sectional area and the channel average velocity. In addition, the tidal excursion was estimated at each site by integrating velocity measurements between slack tides.

Optical Turbidity Measurements

Turbidity, a surrogate measurement for calculating SSC, is a water quality parameter that describes the cloudiness or opacity of the water due to suspended solids (Gray and Gartner 2008). For our measurements, we used YSI, Inc 6920V2 multiparameter water quality sondes that are each equipped with a 6136 optical turbidity probe and self-cleaning wiper (use of firm, trade, and brand names is for identification purposes only and does not constitute endorsement by the US Geological Survey). The sensor readings are in nephelometric turbidity units (NTUs) though our processed data are in formazin nephelometric units (FNUs) based on formazin standard solution calibrations (Rasmussen et al. 2009). FNU complies with USGS guidelines and standard procedures for nephelometric turbidity sensors compliant with ISO 7027 near-infrared wavelength technology (Wagner et al. 2006; Anderson 2004). FNU is essentially equivalent to NTU; the actual SSC was related to the sensor output to obtain a calibration curve as described in Buchanan and Morgan (2010) using a nonparametric slope estimation technique (Helsel and Hirsch 2002).

Suspended-Sediment Concentration Water Sampling

Point-based suspended-sediment concentration (SSC_{pt}) and cross-sectionally averaged suspended-sediment concentration (SSC_{xs}) water samples at all four flux stations were collected during site visits. Point-based suspended-sediment concentration water samples were collected using a Van Dorn sampler at the depth of the turbidity sensor and collected to coincide with the sensor reading at a 15-min interval. The SSC_{pt} samples are coupled with SSC_{xs} to enable comparison of the concentration at the sensor to the cross-sectional average concentration as a means for error checking. The discharge weighted cross-sectional average suspended-sediment samples were collected using the equal discharge increment technique and standard samplers (Edwards and Glysson 1999). Depth-integrated, isokinetic samples were taken from a boat at the centroids of five subsections of equal discharge within each cross-section. SSC_{xs} was regressed against the sensor output, and our result is a 15-min time series of cross-sectionally averaged SSC. All regressions were significant at the 0.000 level, and r-squared values ranged from 0.84 for DWSC to 0.98 for MIN.

Analysis of Suspended-Sediment Flux

Suspended-sediment flux is the product of Q_{xs} and SSC_{xs}. Similar methods have been successfully used to describe sediment flux within the Sacramento–San Joaquin Delta and elsewhere (Wright and Schoellhamer 2005; Ganju and Schoellhamer 2006; Ganju et al. 2005; Wall et al. 2008). Our study design enabled us to use conservation of mass to develop sediment budgets for the study area as an aid

Table 1 Flow meter and index rating information

Site	ADVM frequency (kHz)	ADVM position	AGENCY	Sample/average interval (s)	Index/avg. vel calibration r2
UCS	1,200	Vertical	DWR	300/300	0.987
MIN	1,500	Horizontal	USGS	60/60	1=0.988/2=0.997
DWSC	300	Horizontal	USGS	60/50	0.993
LCS	500	Horizontal	USDs	60/55	1=0.990/2=0.987

The regressions are significant at the <0.001 level. MIN has two ratings (upper and lower). The upper rating for MIN is for ebb tide velocities and the lower is for flood tide velocities towards understanding sediment sources, sinks, deposition, and erosion within our control volume. The boundary of the control volume is defined by our stations and includes Liberty Island (Fig. 2). Sediment accumulation (deposition) or loss (erosion) within the complex was calculated by integrating measured SSF at the control volume boundaries. In this paper, positive and negative values are seaward (down-estuary) and landward (up-estuary), respectively.

The total tidally averaged flux has multiple components and is given by Dyer (1974). Typically, the advective and dispersive components dominate total tidally averaged flux. The advective flux is associated with the mean discharge, while the dispersive flux accounts for tidal pumping and the tidal correlation of concentration and velocity. The combination of both the advective and dispersive fluxes, typically account for more than 90% of the total tidally averaged flux. Stokes drift flux is the tidal correlation of velocity and area and typically accounts for a small portion of the total. For the purposes of this study, we calculate the total tidally averaged flux as the combination of the advective, dispersive, and Stokes fluxes as shown in Eq. 1.

$$[F] = [U][A][C] + [[U'[A]C']] + [[U'A'[C']] \qquad (1)$$

in which U is the cross-sectionally averaged velocity, A is the cross-sectional area, C is the velocity-weighted cross-sectionally averaged suspended-sediment concentration (SSC_{xs}), $[x]$ indicates tidal averaging of variable x, and x' is the deviation of x from the tidal average such that $x=[x]+x'$. A low-pass Butterworth filter with a cutoff period of 30 h was used to compute tidal averages.

The sediment budget at each site for the duration of the study and for each of the 2009 and 2010 water years (WY) was calculated by integrating the 15-min flux values. The total residual flux calculated from the advective, dispersive, and Stokes components was compared to the total residual flux calculated as the product of flow and suspended-sediment concentration (Q* SSC_{xs}) as a means of error checking. The product of flow and suspended-sediment concentration was not used for the sediment budgets.

Data gaps were estimated using multiple methods. There were very few data gaps in the flow records. Only 2 % of the flow data were missing. Suspended-sediment records had larger data gaps representing approximately 10 % of the records due to biological fouling of the turbidity sensors, which required estimation of the flux time series. In order to calculate total flux from Q* SSC_{xs}, flow and flux time series data gaps were filled. Data gaps <3 h were filled by linear interpolation. Data gaps of <1 day were the most common and were manually filled using the preceding or following day's values (i.e., for the estimated value at a given time, the value at either −23 or +25 h was used), based on the similarity of the tides within the spring/neap cycle for each adjacent day. To fill larger gaps within flow records, flow at the site in question was estimated with regression by correlating flow at the next nearest site. Rating curves were developed between flow and suspended-sediment flux to fill data gaps within the flux records. Data gaps were filled piecemeal, meaning that regressions were acquired from the correlations surrounding the time period of the data gap, rather than applying one blanket rating curve to all data gaps. This technique was used because of the tidal (spring/neap) and seasonal variation in flow during the study. These regressions were developed using approximately 3 days of data surrounding each gap. A longer window did not improve residuals. R^2 exceeded 0.90 for all rating curves. The data gaps in the advective, dispersive, and Stokes flux cumulative records were individually interpolated from the mean change in cumulative sediment flux (mean slope) preceding and following each data gap. On average, these interpolated estimations represent 12 % of the flux (Table 3). The difference in total computed flux from a comparison of both methods was <3% on average. Although UCS had the largest percent flux estimated (24 %), it only represented 2.1 kt (Table 3).

Additional Data

Hourly wind speed data (sites shown on Fig. 2) were obtained from the California Irrigation Management Information System (http://www.cimis.water.ca.gov). We utilized additional turbidity data from 15 sites throughout the Delta (maintained by the California Department of Water Resources Environmental Monitoring Program) in order to compare the turbidity in the Cache Slough complex with the rest of the Delta. Precipitation and the DWR turbidity data was downloaded from the Department of Water Resources California Data Exchange Center (CDEC) http://cdec.water.ca.gov/. Solano County Water Agency (SCWA) measures turbidity and discharge in Lindsey Slough (site LSHB, Fig. 2). Data from this site were acquired directly from SCWA.

Results

Cache Slough Complex and Delta Turbidity

Our results confirm that the Cache Slough complex in the north Delta is more turbid than the rest of the Delta. The mean turbidity at five locations (our four sites plus Lindsey Slough maintained by Solano County Water Agency) was compared to all other available Delta turbidity data, throughout 2009 and 2010. Turbidities were twice as high in the study area (mean, 27 NTU) compared to elsewhere in the Delta (mean, 13 NTU) (Fig. 3).

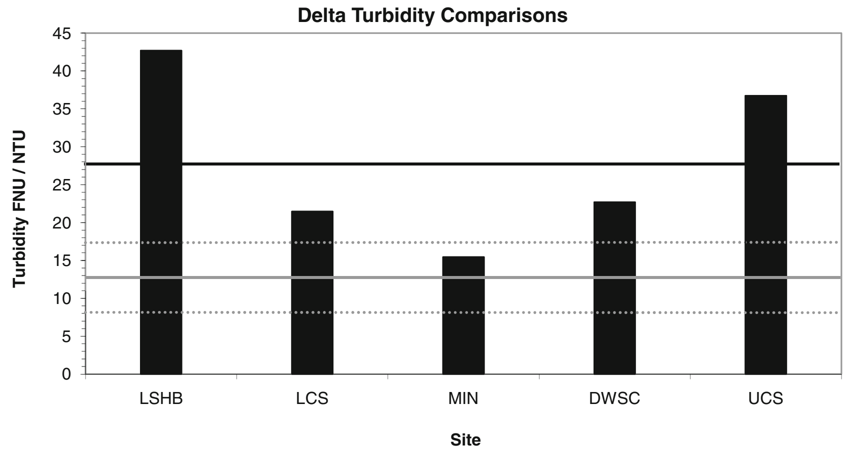

Fig. 3 Average turbidities for 2009 and 2010 within the Cache Slough complex (*black line* represents mean) compared to the Delta mean (*solid gray line*)±1 standard deviation (*dotted gray lines*)

Tidally Influenced Water Discharge

All locations within our study area are influenced by tides, but there is a diminishing effect as distance upstream increases (Fig. 4a). LCS has the largest bidirectional flow and MIN has the largest cumulative seaward flow. During the dry season, UCS and DWSC have minimal cumulative seaward flow. LSHB (Lindsey Slough) has minimal cumulative seaward flow (data not shown), and cumulative landward flow at LSHB is enhanced by the water pumps on Barker Slough. MIN is mostly bidirectional, yet not all flood tides are strong enough to reverse flow at the site. Flow at MIN may remain unidirectional seaward for more than 1 month during large flow pulses from the Sacramento River watershed. During this study, there were two flow pulses at MIN, unlike the other sites. Large winter flow pulses occurred at the beginning of February 2009 and in January of 2010. The peak discharge at MIN during the study period was in January 2010 (261 $m^3 s^{-1}$). The range in water velocity within the study area was between 95 $cm s^{-1}$ (ebb) and 90 $cm s^{-1}$ (flood). The fastest current was at LCS with mean of 49 $cm s^{-1}$, and the smallest mean current speed was at UCS, which was approximately 6 $cm s^{-1}$.

Flood Dominant Velocities and Sediment Transport

Velocity statistics are shown in Fig. 4b. Estuarine tidal asymmetry can be described by comparing the tidal period and tidal velocities, where a flood dominant channel has a shorter duration, higher velocity floodtide, and an ebb dominant system has a shorter, higher velocity ebb tide (Friedrichs and Aubrey 1988). Median flood tidal period is shorter than median ebb tidal period (Table 2). Landward of LCS, the channels surrounding Liberty Island have higher velocities in the flood direction than ebb (Table 2). MIN is an exception to this because this site has more influence from the Sacramento River and is ebb dominant. Furthermore, the sediment transport capacity of the flow was inferred by analyzing the velocities cubed. Sediment transport scales with shear stress to the 1.5 power, and shear stress scales to velocity squared, so sediment transport roughly scales to velocity cubed. The flood/ebb ratio of cubed velocity shows that the ability for the flood tide to transport sediment (Son and Hsu 2011) in the landward direction is twice that of the ebb tide for both the DWSC and UCS sites (Table 2), consistent with the landward cumulative flux observed at those sites. The flood/ebb ratio at LSHB and Liberty Island also indicated flood dominance (data not shown), and we would expect that sediment flux is landward. Although the flood and ebb velocities at LCS are nearly equal, during low freshwater flows typical during summer and fall, the peak velocities occur during the flood tide and coincide with high sediment concentrations enabling a landward flux. This tidal variability is similar at all sites (except MIN). The peak ebb velocity coincides with

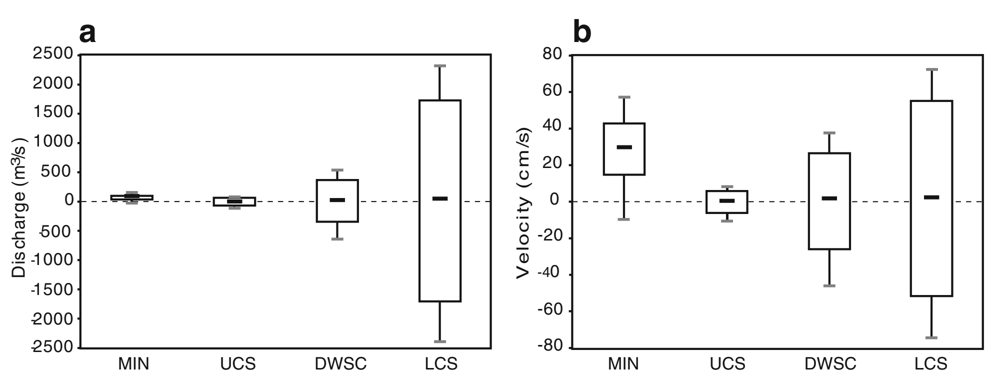

Fig. 4 Flow statistics box plot (**a**) and velocity statistics box plot (**b**). The bars are the 5th and 95th percentiles, the *boxes at the top and bottom* are the upper and lower quartiles, and the *line inside the box* shows the median

Table 2 Tidal excursion and velocity statistics

Site	Tidal excursion (km) flood/ebb	Tidal period (h) ebb/flood	Mean velocity n(cm s−1) flood/ebb	Velocity 95th percentile flood/ebb	V3 f/V3 e
UCS	1.2/1.2	7.0/5.25	−6.4/5.4	−12.2/8.8	2.0
MIN	1/12	12.0/3.5	−9.7/33.4	−19.6/63.4	0.02
DWSC	5.1/5.9	8.25/4.75	−61.9/51.2	−50.0/39.3	1.8
LCS	10.4/12.8	7.25/5.25	−49.1/48.9	−77.4/75.2	0.9

Positive values indicates seaward direction

a smaller concentration of suspended sediment. During ebb, the sediment is advected downstream, and high concentrations of sediment occur at the end of ebb when the velocities are low. Therefore, high sediment concentrations also occur at the beginning of flood tide. The peak concentrations that coincide with peak flood tide velocities are indicative of resuspension (Fig. 5).

Sediment Supply from Watersheds

Miner Slough is a significant source of sediment to the Cache Slough region. Miner Slough captures approximately 20% of the water from the Sacramento River. After sufficient rains have fallen to saturate soils or when the precipitation intensity is such that it exceeds infiltration rates within the watershed, a winter storm will initiate runoff erosion and mobilize bed sediment, transporting it down the Sacramento River. The first flush is the initial surface runoff from a rainstorm following the dry period and flushes typically higher sediment concentrations than subsequent storms. Additionally, the peak concentration typically precedes the peak flow. An increase in sediment concentration depends on multiple factors such as storm and watershed conditions, but throughout this study, when the flow exceeded 560 $m^3 s^{-1}$ in the Sacramento River, there was an increase in sediment concentration into Miner Slough. An example of a first flush is shown in Fig. 6 where the first significant surface runoff (February 2009) flushed a higher sediment concentration (peak SSC, 306 mg/L) than subsequent flows (May 2009) (peak SSC, 84 mg/L). The peak concentration occurred in February, whereas the peak flow occurred in March. The first flush sediment pulses within Miner Slough, throughout the study, occurred when there was a sudden increase in flow along the Sacramento River to >1,000 $m^3 s^{-1}$, and within the time frame of this study, these were the largest sediment pulses.

The other major source of watershed sediment is Ulatis Creek, which delivers sediment from the Coast Range as well as urban and agricultural runoff. The smaller (4,500 km^2) Ulatis Creek watershed responds more rapidly than the larger

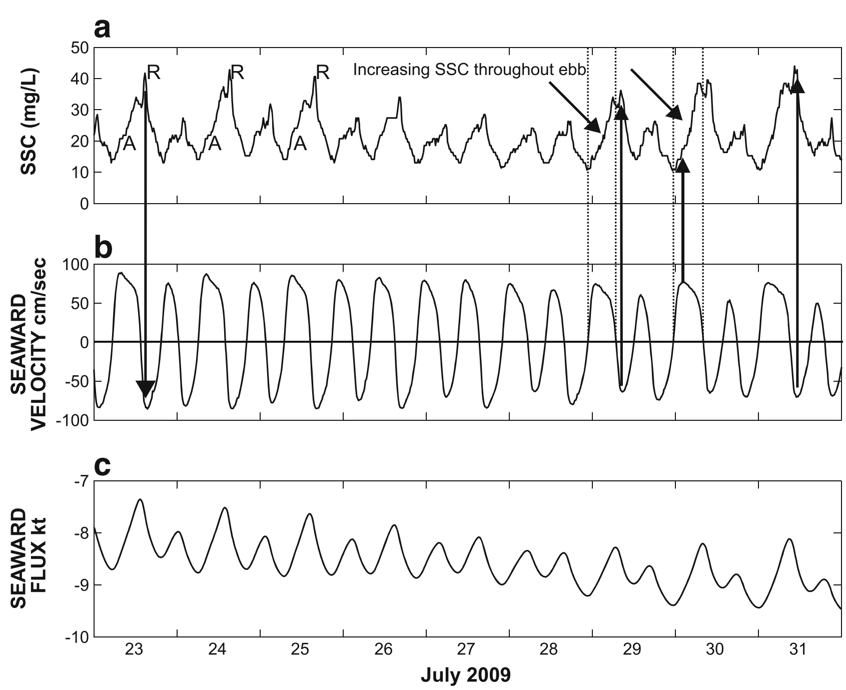

Fig. 5 Average cross-sectional suspended-sediment concentrations (**a**), velocity (**b**), and seaward flux in kilotons (**c**) for LCS during July 23 to July 31, 2009. Advection (*a*) and resuspension (*R*) are shown in *top panel* (**a**). The *dashed lines* and *diagonal arrows* highlight increasing SSC throughout the ebb as labeled in figure. The *vertical arrows* point out both minimum SSC correlated to peak ebb tide velocity, and maximum SSC correlated to peak flood tide velocity

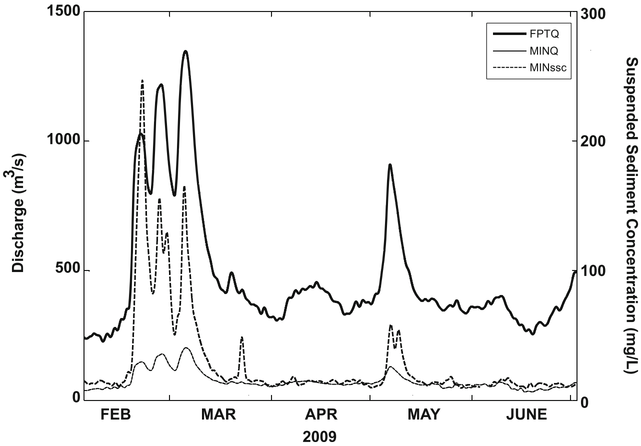

Fig. 6 The first flush concept shown for Miner Slough during 2009. FPTQ represents the flow in the Sacramento River at Freeport

(70,000 km^2) Sacramento River watershed. An example of this is shown in Fig. 7 during October 2009. A storm produced 76 millimeters of rain within 24 h after which a sediment pulse came into the complex from the west and was observed at UCS. Sediment concentration did not increase at MIN. Turbidity at UCS remains elevated as higher concentrations of sediment move seaward, deposit on slack, get resuspended at the initiation of the flood tide, and move back upstream. Some of this sediment arrived downstream at LCS (arrow, Fig. 7). On the subsequent flood tides, some of this sediment is pushed back upstream and was observed at the DWSC site. Travel time of the suspended-sediment pulse from UCS to LCS and DWSC (8.2 and 4.9 km, respectively) was 14 days due to limited tidal excursion.

Sediment Budget and Flux Summary

The cumulative sediment flux for each site is shown in Fig. 8. Over the duration of the study, UCS and DWSC had landward fluxes, but MIN and LCS had seaward fluxes (Table 3). The total net seaward flux for UCS was −8.78 kt, DWSC −8.74 kt (Fig. 8a), MIN 202 kt, and LCS 45.7 kt (Fig. 8c). The overall cumulative flux for LCS was seaward due to the larger seaward pulse during the 2010 storm, although the 2009 net cumulative flux prior to that storm was landward. Generally, the direction of the residual flux differs by season (wet vs. dry) for all sites except for MIN (see Fig. 8b for reference to river flow pulses). Miner Slough contributes sediment to the Cache Slough area throughout the year (i.e., there is a seaward flux throughout the year). Miner Slough delivered significant sediment to the study area (originating from the Sacramento River) during flow pulses in February 2009 and a larger pulse in February 2010 (Fig. 8, MIN, Table 3). During these winter pulses, MIN discharge and sediment flux becomes unidirectional seaward and approximately 60% of the total annual SSF at MIN occurs during this time. Otherwise, Miner Slough delivered a smaller but consistent quantity of sediment to the study area throughout the year (positive slope in Fig. 8). The 2010 total storm flux for MIN was double that of 2009 (Table 3), yet the mass of sediment deposited within the control volume was roughly equal. Approximately 90% of the total calculated influx to the complex came from Miner Slough.

A portion of the sediment observed within Miner Slough is also observed at LCS (the seaward boundary of the study

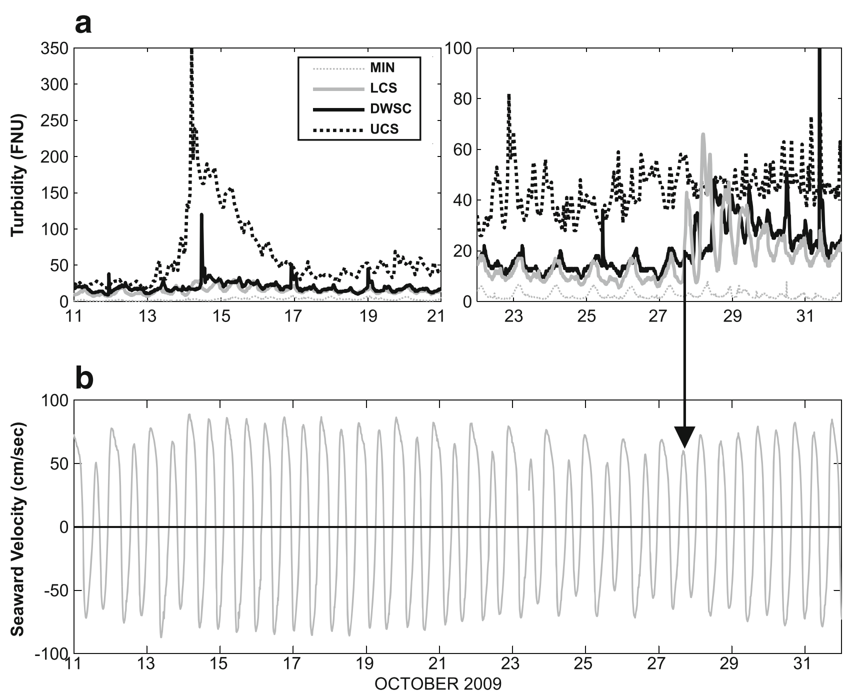

Fig. 7 Sediment concentrations at four stations from a sediment pulse during October 2009 (**a**)—note the two separate *y*-axes. Seaward velocity at LCS is shown in **b**. The *arrow* shows when LCS sediment increased on ebb likely as sediment from Ulatis Creek arrived. DWSC SSC increases on subsequent flood tides

Fig. 8 The cumulative seaward sediment flux within the study area shown in kilotons for UCS and DWSC (**a**) MIN and LCS (**c**), note differing axes. Flow for the Sacramento River is also shown (**b**) for reference to step changes

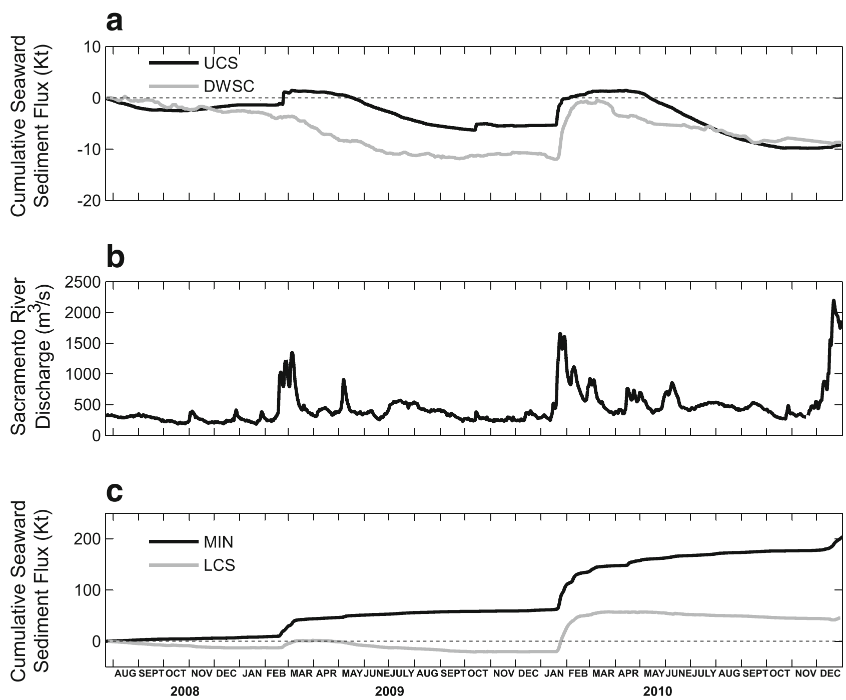

area). Cumulative sediment flux at LCS demonstrates a similar pattern as at MIN (Fig. 8c), though sediment flux patterns from approximately May–October differ between these two sites. During the larger flow pulses, sediment was predominantly exported seaward. Otherwise, sediment transport was landward at LCS (negative slope in Fig. 8c), indicating that sediment was trapped within the study area when freshwater inflow was low.

The storm runoff sediment pulses observed at UCS are initiated from the Ulatis Creek watershed compared to the sediment in Miner Slough that initiates from the Sacramento River Watershed. Rainfall induced runoff from Ulatis Creek is flashy in character. As mentioned previously, the sediment pulse and small seaward flux observed at UCS in October 2009 (Fig. 7) was not observed at MIN and LCS, nor was the storm large enough to trigger increased sediment concentrations from the Sacramento River watershed. The net sediment flux at sites UCS and DWSC was much smaller than MIN and LCS and usually landward in direction. The primary flow pulse of 2009 at UCS produced half as much sediment as the 2010 first flush (Table 3). At DWSC, the first flush pulse was landward in 2009 and seaward in 2010. The effect of Ulatis Creek, influenced by agricultural runoff, was marked by an increase in salinity values at UCS and Ulatis compared to downstream sites, especially during the ebb tide.

Flux Decomposition

Advective and dispersive fluxes dominate sediment transport at all sites (Table 3). The advective flux dominates the total flux at MIN and accounts for 95 % of the sum of the magnitudes of the advective, dispersive, and Stokes components (Fig. 9, Table 3). The magnitude of the landward flux components divided by the sum of the component flux magnitudes increases landward from 43 % at LCS to 53 % at DWSC to 85 % at UCS (Table 3). Thus, sediment is more effectively trapped at sites landward of LCS (with exception of MIN).

At UCS, the combination of advective and dispersive fluxes account for 99 % of sum of the component flux magnitudes (Fig. 9, Table 3). For DWSC and LCS, the

Table 3 Calculated fluxes for study period July 23, 2008 through December 2010

Site	2009 first flush	2010 first flush	Total sediment flux (kt)/% est.	Advective flux (kt)	Dispersive flux (kt)	Stokes flux (kt)
UCS	2.66	6.53	−8.78 (import)/24	−10.73	1.88	0.07
MIN	32.42	82.35	202.11 (export)/1.7	198.21	6.94	−3.04
DWSC	−0.51	11.64	−8.74 (import)/15	62.12	−61.18	−9.68
LCS	13.70	75.06	45.70 (export)/6	197.31	−122.03	−29.58

We calculated the flux for the first flush that occurred from February 18 to March 15, 2009 and during the flow pulse from January 15 to February 18, 2010. Positive values indicate seaward transport

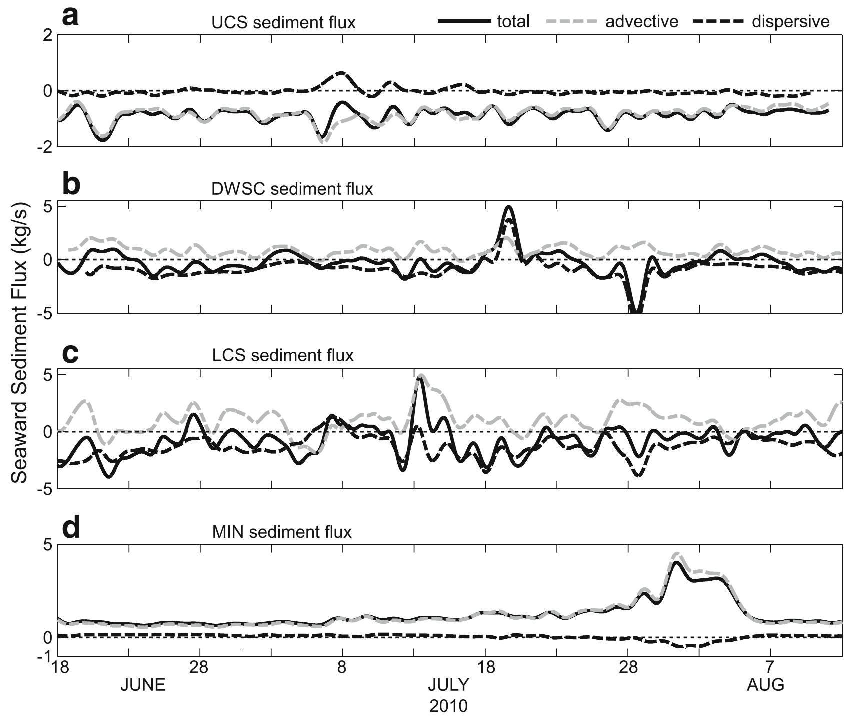

Fig. 9 Total, advective, and dispersive fluxes shown during June 18 to Aug 12, 2010 for each of UCS (**a**), DWSC (**b**), LCS (**c**), and MIN (**d**). Positive values represent seaward flux, and negative values represent landward flux

combination of advective and dispersive fluxes account for roughly 92 % of the sum of the component flux magnitudes, but the contribution to the total varies seasonally. During the winter, the flux is primarily seaward during increased freshwater flow pulses following storms (Fig 8) and the advective residual flux dominates. From approximately May through October, the net flux is landward at all sites but MIN. A low flow example of all sites from June through August 2010 is shown in Fig. 9. During this time, freshwater flow is at a minimum and the dispersive flux dominates at both LCS and DWSC, transporting sediment landward where it is further trapped within the Cache Slough region. For example, at LCS from May to October, 78 and 62 % of the sum of the component flux magnitudes was landward during WY 2009 and 2010, respectively (2010 shown in Fig. 10). In other words, on average, 70 % of the sum of the component flux magnitudes from May to October was landward at LCS compared with December to March when 73 % was seaward. From May to October, the sediment flux was landward due to the combination of dispersive and Stokes fluxes despite the fact that net discharge was seaward.

At UCS, the predominant landward flux was due to advection and could not be explained by replenishment of water lost to evaporation. Irrigation pumping may anthropogenically enhance the advective flux during the growing season. The irrigation diversion capacity on Hass Slough is approximately 9.2 m^3/s (Solano County Water Agency, personal communication). At UCS, typical tidal flows are approximately 60 $m^3 s^{-1}$, and tidally averaged flow from March through September is −10.2 m^3/s landward, similar to the Hass Slough diversion capacity. Diversions on other sloughs landward of UCS and pumping at less than capacity may account for the 1 m^3/s difference between measured flows and Hass Slough diversion capacity. Irrigation diversions are likely the cause of the large landward advective flux at UCS that we observe during the growing season.

Limited Tidal Excursion

We found that the channels surrounding Liberty Island have tidal excursions smaller than the channel lengths (excluding MIN) (Fig. 11). This prevents sediment in much of the study area from exiting during ebb tides. The UCS site has the smallest tidal excursion compared to all other sites. The seaward tidal excursion during the average ebb tide is only 1.2 km and does not reach the confluence of other channels or to Liberty Island and is only slightly more than one tenth the distance to the seaward boundary of the study area (LCS). The suspended sediment at UCS essentially oscillates back and forth with the tides. Thus, suspended sediment at UCS is not flushed out of the study area during an ebb tide and sediment that is transported to UCS during a flood tide is trapped.

The tidal excursion of the DWSC and LIB sites from an average ebb tide can reach the seaward boundary of the study area (LCS), yet only towards the end of the tide, and therefore, the high concentrations of sediment that are seen at the end of the ebb (Fig. 5) are transported back into the study area at the beginning of the flood tide. Although the ebb tidal excursion from LCS is more than 12 km and reaches Rio Vista, small

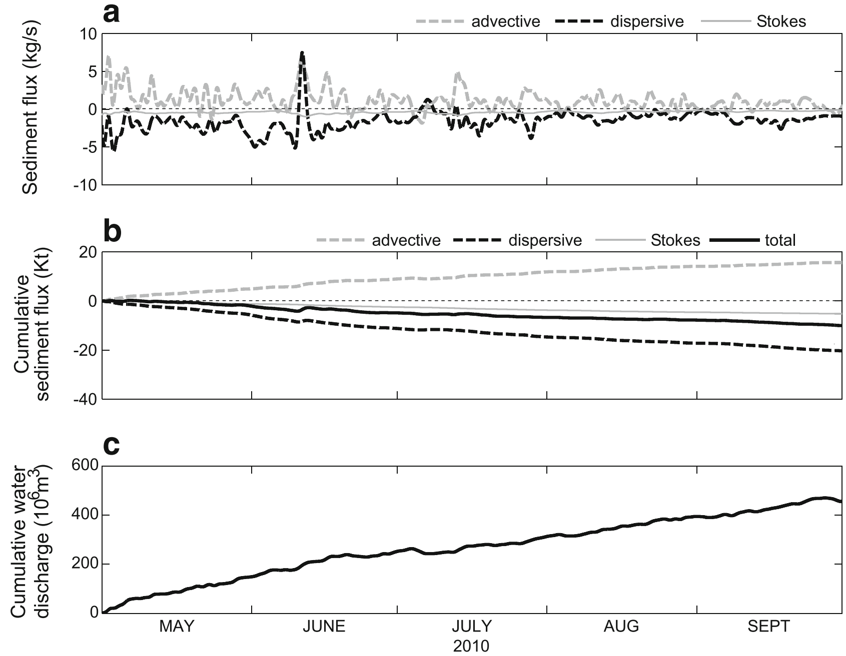

Fig. 10 The sediment flux characteristics at LCS during the low flow period of May through September of 2010. Residual advective, dispersive, and stokes flux (**a**), the cumulative sediment flux in kilotons (**b**), and the seaward cumulative discharge (**c**)

suspended-sediment concentrations that are observed at the beginning of ebb are transported at this distance compared to the higher concentrations that are advected to LCS a the end of ebb tide (Fig. 5). The smallest SSC occurs at the end of flood tide from clearer water that is from downstream of the complex and moves in with the flood tide.

Discussion

We found that the Cache Slough complex is characterized by the presence of a turbidity maximum zone. Freshwater pulses supply sediment to the complex and some of that sediment is exported seaward (Table 3, first flush). During predominant low flow conditions, wind–wave resuspension, tidal asymmetry and limited tidal excursion all contribute to net landward sediment flux and trapping of sediment in the complex, which maintains the turbidity maximum. We discuss these drivers of the Cache Slough complex in the following paragraphs.

Turbidity Maximum in a Backwater Tidal Slough Complex

Multiple researchers have noted the accumulation of suspended material within estuarine turbidity maximum (ETM) at the upper end of an estuary at the freshwater/saltwater interface (Wolanski et al. 1995; Roman et al. 2001; Schoellhamer 2001; Kitheka et al. 2002, 2005; Tattersall et al. 2003; Uncles et al. 2006) and estuaries can have multiple ETMs (Jay and Musiak 1994). ETMs are commonly associated with the salinity field, but other factors can create and maintain ETMs. Conditions necessary for a turbidity maximum in a tidal system include a supply of erodible sediment and a mechanism to retain suspended sediment at a specific location. Topography can also influence the formation of an ETM (Jay and Musiak 1994). Schoellhamer (2001) documented a topographically controlled ETM within the San Francisco Estuary at the eastern edge of Carquinez Strait and western Suisun Bay. Ganju et al. (2004) observed turbidity maxima in two single tidal channels in San Francisco Bay that were predominantly a function of tidal currents and spring/neap variability. Relatively high turbidity in the Cache Slough complex (Fig. 3) indicates the presence of another ETM within the estuary. Winds (Weir and McManus 1987; Uncles and Stephens 1993, 2010; Wolanski et al. 1995; Schoellhamer 1995), tidal asymmetry (Hamblin 1989; Dronkers 1986; Jay and Musiak 1994; Sanford et al. 2001), and low freshwater flow are physical drivers that account for a landward turbidity maximum seen in the Cache Slough complex. These processes efficiently trap sediment within the shallow dead end sloughs and Liberty Island. We see a concentration gradient and sediment convergence within this backwater area (Fig. 12); it is only episodically flushed.

Supply and Export of Sediment

A supply of erodible sediment is needed to create an ETM. Cache Slough is a complex system with two main sources of fine and erodible sediment, Miner Slough and Ulatis Creek. These tributaries supply sediment to the complex annually. The Deep Water Ship Channel ends at the Port of Sacramento and the flooded Liberty Island is dry to the north. UCS directly receives sediment from Ulatis Creek, and Miner Slough receives sediment from the Sacramento River. The major source of sediment into the complex is from Miner Slough,

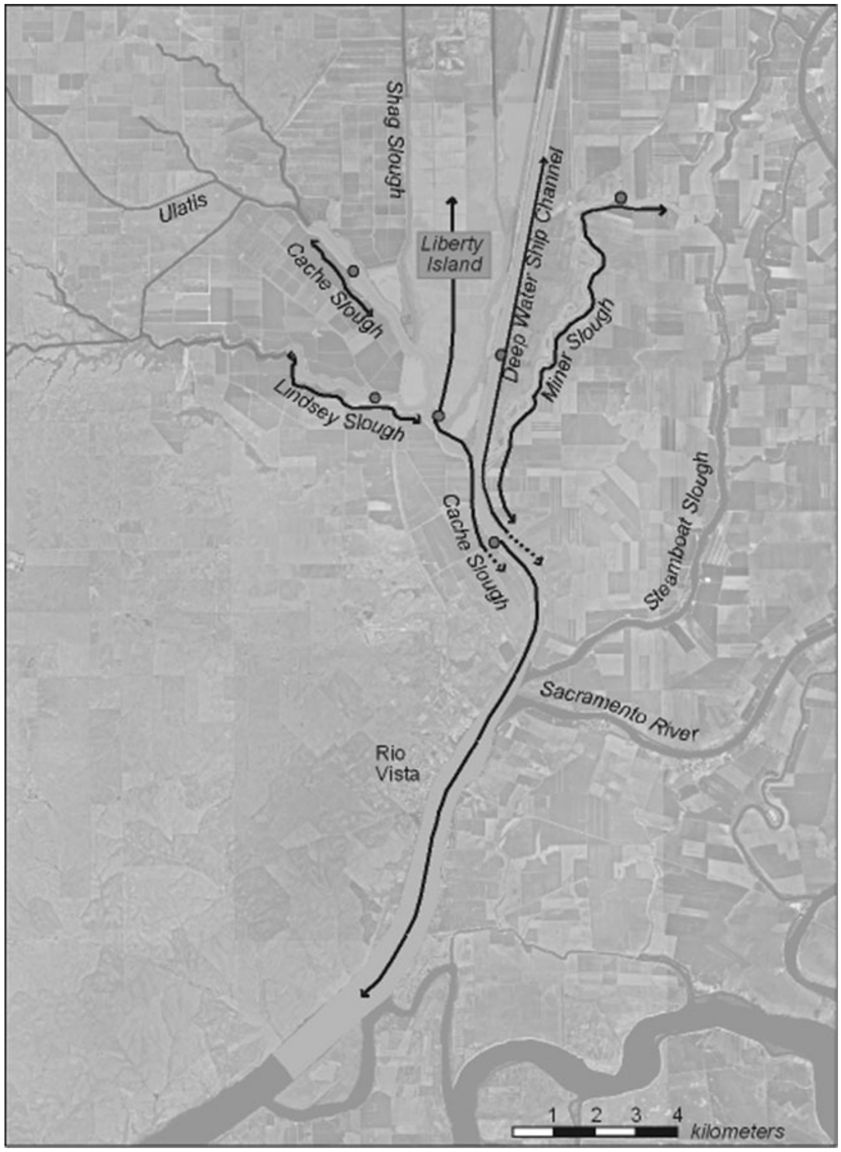

Fig. 11 The extent of the mean tidal excursion is shown for six sites within study area including Lindsey Slough and Liberty Island. The excursions are shown with *black lines* and *arrows* to represent the landward/seaward limits from each station (represented by *circles*). Refer to the landward sites for the excursion above LCS

approximately 65% of which occurs during the episodic first flush event. DWSC (Fig. 7a, right) and Liberty Island (Fig. 13b) predominantly received sediment during flood tides. As mentioned previously, Fig. 7 shows an isolated sediment pulse into the system from Ulatis Creek during October 2009. Although the net flux at LCS was seaward during this event, more than 60 % of the sediment was retained. This sediment pulse was not completely flushed out of the complex. Turbidity is greater at UCS than DWSC (Fig. 3), both because of its relation to Ulatis and because of its tidal isolation (Fig. 11).

Although the Liberty Island data did not encompass the entire time period of the study, we were able to observe that, enhanced by tidal asymmetry, it is possible that sediment is transported into Liberty Island during and/or immediately following episodic events. The data is consistent with that of other sites and shows tidal asymmetry, a concentration gradient, and that sediment transport is limited by the tidal excursion. During low flow, turbid water leaves the island on ebb tide (Fig. 13a), and during episodic events, turbid water enters the island on flood tide (Fig. 13b). Depending on the discharge during the event and where the increased sediment concentration initiates from, it is possible that sediment moves into Liberty Island and deposits. In other words, a pulse of sediment may come from MIN and/or UCS and can be transported into Liberty Island during the flood tide. Here though, we note that there may be deposition when floodwaters are routed through the Yolo Bypass, but no such events occurred during the time period of this study. Furthermore, it is also possible for sediment in Cache Slough to be transported into Liberty Island during the flood tide in low flow summer months.

During low flow periods (approximately 75 % of the time when freshwater inputs are at a minimum and mean daily flow is typically much <400 $m^3 s^{-1}$ at MIN), there is net

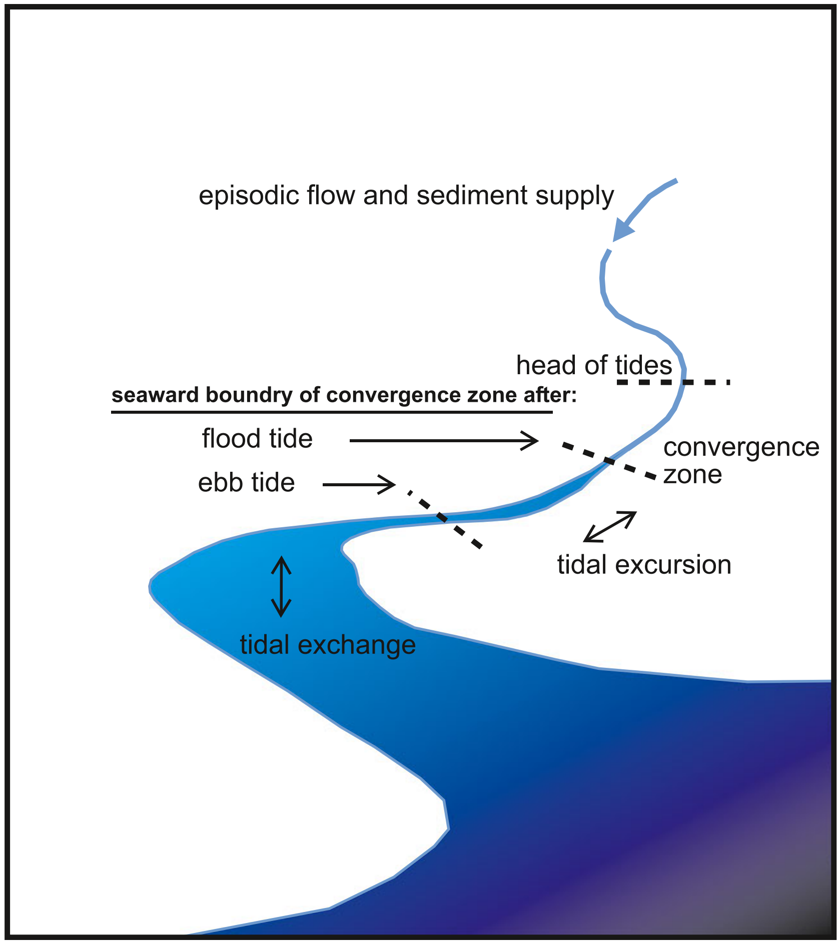

Fig. 12 Conceptual diagram of sediment convergence at the landward boundary of the estuary

outflow of water from Cache Slough at LCS, but the sediment flux is landward (Fig. 10) and high sediment concentrations remain localized. Furthermore, the net sediment flux from approximately April to October is landward at all sites, except at MIN, which continues to supply sediment into the complex—all of which is retained. Sediment accumulation into the study region at LCS is enhanced by flood dominant velocities and retention is due in part to the limited tidal excursion.

Episodic flow from the watershed deliver both freshwater and sediment. Episodic flows also reduce residence time and flush the system. The extent of which the system is flushed of sediment is dependent on the size of the flow pulse. It is possible for some sediment to be retained during a large event. Deposition within the control volume during a first flush is a function of the water discharge and sediment supply. At the landward end of an estuary, a freshwater pulse can convert channels that typically experience bidirectional flow to unidirectional seaward flow. The discharge and duration of unidirectional flow may limit deposition within the control volume. For example, during the 2010 first flush (January 14–March 15), twice as much sediment came into the area from MIN compared to 2009 (February 13–March 26), but only 25 % was retained compared to approximately 60 % in 2009. Over the duration of study, the net sediment flux from the complex was seaward because of large episodic flows that flushed the system (LCS Fig. 8).

There may be an optimal water and sediment discharge for sediment deposition in an estuarine backwater zone. As the size of the flushing pulse increases, sediment supply and erosive forces will increase. The actual sediment mass retained in the system was nearly equal for 2009 and 2010 (21 and 25 kt, respectively), but the total mass supplied from MIN was more than double in 2010 (32 vs. 82 kt). The unidirectional freshwater flow pulse from MIN during 2009 extended 40 days and the SSC peak occurred during a flow of 170 m^3/s compared to 2010 extending 65 days with the SSC peak occurring during a flow of 260 m^3/s recorded at MIN. The 2010 discharge was 35 % larger in the Sacramento River and Miner Slough than 2009 during the primary sediment pulse. The net sediment supplied from Miner Slough was twice as much in 2010 (117 kt) than in 2009 (54 kt).

Net deposition depends on the geomorphic characteristics, water discharge, and associated sediment supply. Depositional areas include dredged channels, tidal marsh, shoals, and flooded islands. Potential erosional areas include channels that experience greater ebb currents during pulses.

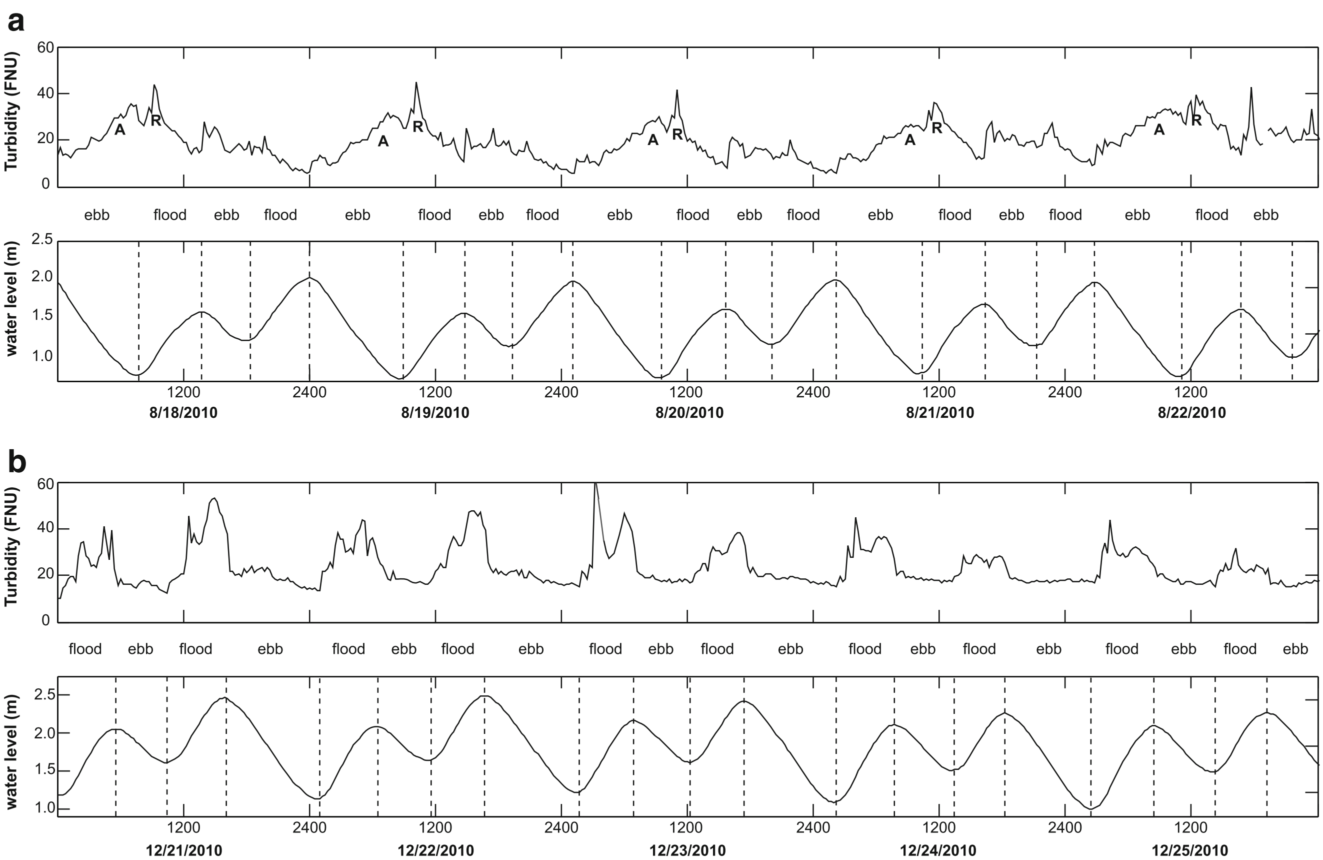

Fig. 13 Liberty Island turbidity and tides during the dry season from August 18–22, 2010 (**a**) and during high flow from December 21–25, 2010 (**b**). Advection (*a*) and resuspension (*r*) are shown in the *top panel*

One extreme bound is if there are no depositional areas in an estuarine backwater zone, for which a pulse can only erode sediment and erosion will increase as water discharge increases (Fig. 14). Another extreme bound is if there is unlimited depositional area such that, as water discharge and sediment supply increase, deposited mass will increase. Between these extreme bounds, as depositional areas fill with sediment, or if the rate at which sediment can enter a depositional area is constrained (a high tidal marsh or a small levee breach at a flooded island), supplied sediment cannot be stored. As discharge and sediment supply increase, deposition would be constant or decrease while erosion increases, leading to a conversion from net deposition to net erosion (Fig. 14). In this case, there is an optimal water discharge that maximizes sediment deposition. As the ratio of depositional to erosional areas increase, the mass of sediment deposited by a given pulse will increase, assuming all other factors are equal.

During the time period of the study, we did not see extreme sediment erosion. Liberty Island is at the southern end of the Yolo Bypass. Discharge from the Yolo Bypass will flow through Liberty Island downstream to LCS. Typical peak discharge from the Yolo Bypass (1,400–10,500 $m^3 s^{-1}$ not observed during our study) likely exceeds the first flush discharge that we observed at Miner Slough by a factor of 5–25. Additional data is required to determine sediment retention during these flows.

For the Cache Slough complex, mass deposition in 2009 and 2010 were nearly equal, with a much larger water discharge during the first flush pulse in 2010. Based on only 2 years of data, to maximize deposition within the complex, a discharge less than that of 2010 seems necessary. In addition, in 2009, the sediment flushed in the winter was

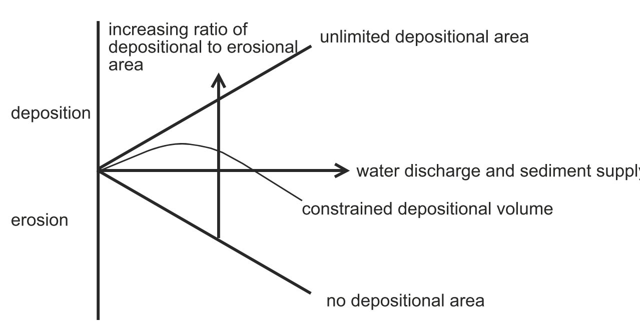

Fig. 14 Conceptual diagram of net deposition or erosion in an estuarine backwater zone near the landward boundary of the estuary as a function of water discharge and sediment supply

completely replenished to the system throughout the following spring and summer. The perimeter of Liberty Island is 25 km, and the main south breach is 200 m wide; it is therefore likely that sediment delivery to Liberty Island during large pulses, especially from Yolo Bypass, is constrained. Substantially smaller water discharges likely would deposit less sediment and larger water discharges likely would export sediment from the complex and into the San Francisco Bay.

Wind–Wave Resuspension Enhances Sediment Concentrations

Wind–wave resuspension is a mechanism for erosion of sediment from shallow water (Uncles and Stephens 1993, 2010; Wolanski et al. 1995; Schoellhamer 1995). Wind-induced waves enhance bed turbulence and cause an increase in bottom shear stress, which can cause sediment resuspension and enable tidally transported sediment to remain in suspension (Jing and Ridd 1996). Increased sediment resuspension from wind is an important factor for suspended-sediment concentrations in the San Francisco Bay (Krone 1979; Schoellhamer 1996; Brand et al. 2010), in Cleveland Bay, Australia (Jing and Ridd 1996), as well as The Chesapeake Bay (Ward 1985), as a few examples. Additionally, sediment deposited during the winter within the Cache Slough area is available as unconsolidated material that is subject to wind–wave resuspension. Sediments undergo tidal and wind–wave resuspension, which maintains turbidity throughout the region.

During the spring and summer months, increased onshore winds penetrate throughout the Delta. The sediment concentrations notably increase during this time (Fig. 15). Figure 13 supports the concept that Liberty Island is an important sink of erodible sediment for subsequent wind–wave sediment resuspension. It is common that Liberty Island accumulates sediment during winter sediment pulses; the turbidity increases by a factor of 2 during the flood tide from December 21 to 25 (Fig. 13b). The turbid nature of Liberty Island is enhanced by wind–wave resuspension of the erodible sediment within this shallow flooded island. Increased sediment concentrations within Liberty Island from wind–wave resuspension are advected seaward during ebb tides and enhance the turbidity within the study region. Increased sediment concentrations during the ebb, typical of the dry season, are shown in Fig. 13a.

DWSC, UCS, and Ulatis Creek all have shallow areas in their cross-sections. Specifically, two thirds of the DWSC cross-section is <6 m deep, and more than half the channel is <2 m deep. Ulatis Creek and UCS both have shallow within channel shoals. The highest turbidities and sediment concentrations, excluding the winter pulse, occur during late spring and summer when wind speed is the greatest. This time coincides with the largest landward flux at the landward boundaries of the study area (negative slope of cumulative flux at UCS and DWSC in Fig. 15a). Increased SSC at UCS correlated to increased wind speed (Fig. 15b, c). This is evident at other locations such as LCS where the baseline SSC is typically higher in May, June, and July. During these times, we observed resuspension of the fine and erodible sediment, causing larger SSC.

Tidal Asymmetry

Flood dominant velocities are one of the mechanisms of trapping sediment in the landward ends of the Cache Slough complex. The velocities at UCS, DWSC, and LSHB were generally larger in the flood direction (Table 2). Peak velocities at these sites (excluding the winter pulse) occur during the flood tide, which creates an asymmetry in both bed shear stress and sediment flux. It is typical for peak suspended-sediment concentrations to coincide with the peak flood velocity (Fig. 5). Maximum flood velocities during a spring tide at UCS, for example, are typically around 15 $\mathrm{cm\,s^{-1}}$ compared to 9 $\mathrm{cm\,s^{-1}}$ during the ebb. Comparatively, the largest suspended-sediment concentrations during the ebb occur at the end of the larger ebb tides, most likely due to seaward advection of more turbid water. Advection of sediment downstream during the ebb and peak sediment concentrations during the flood are observed at most sites (Fig. 5a and 13a).

Limited Tidal Excursion

Another key sediment retention mechanism is the limited tidal excursion, which retains water and sediment in the Cache Slough system at the end of ebb tide. The more landward regions of the complex have a small tidal excursion during low freshwater flow (Fig. 11). Most of the water and sediment in the system at the beginning of ebb tide remain in the system at the end of the ebb tide. The mass of sediment that is mobilized from UCS does not reach LCS on an ebb tide (Fig. 11). Only about 60 % of the ebb tides are adequate to move sediment from the DWSC site to LCS; the tidal excursion for weaker ebbs and neap ebbs are less than the 4.9 km distance between the sites. For weaker ebbs, the excursion does not reach the lower limits of the Deep Water Ship Channel where it meets Cache Slough. Therefore, not all sediment leaves the Deep Water Ship Channel and not all sediment is mobilized to reach LCS. Furthermore, during a stronger spring ebb tide, only an average 35 % of the total sediment mass from the DWSC site will reach LCS. This is because the sediment moving past the DWSC site during the latter part of the ebb does not reach LCS before the subsequent flood tide. The small percentage of sediment that is

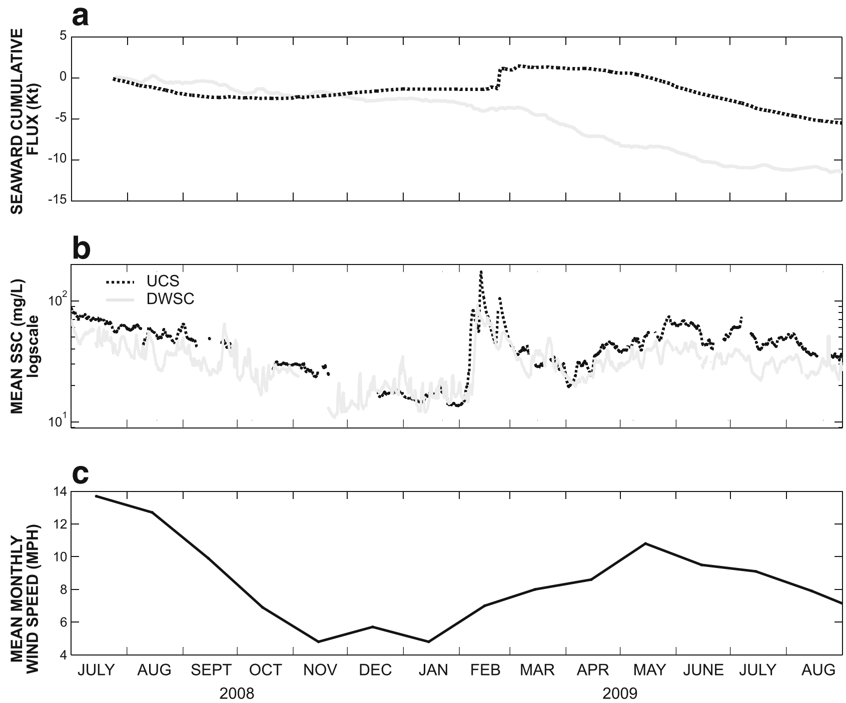

Fig. 15 Cumulative flux for UCS and DWSC (**a**), suspended-sediment concentration (**b**), and mean monthly wind (**c**) July 2008 through August 2009

mobilized downstream to LCS is pushed back upstream on the subsequent flood tide. This repeated pattern during the dry season enhances cumulative landward sediment transport at LCS. In summary, Cache Slough contains a turbidity maximum because it is supplied with erodible sediment that is retained by flood dominant velocities and a limited tidal excursion.

Tidal Trapping and Convergence of Sediment in the Backwaters of the Estuary

Two key physical characteristics of the Cache Slough complex are that (1) tidal excursions are small enough compared to the length of the system that a large fraction of the water volume (and sediment) is retained in the system after ebb tide and (2) flood-tide dominant currents. Tidal marsh habitats surrounded by dead end sloughs used to be common in the Delta (Grossinger and Whipple 2009) but are now rare habitat. Much of the Delta is now connected waterways with little isolation. The isolated nature of the Cache Slough backwater area, which includes dead end sloughs, enables retention of sediment and greater turbidity in areas such as Liberty Island.

Conclusions

During this study, we obtained a continuous record of suspended-sediment concentrations and described the timing and transport mechanisms within the Cache Slough Complex. The Complex is predominantly isolated and episodically flushed. Sediment trapping is caused by tidal asymmetry, low fresh water flow, and a limited tidal excursion. The upper reaches of the dead end channels in the study area are dominated by flood tide velocities. From spring to the end of summer/early fall, when the downstream river flow is not dominated by precipitous winter storms or significant snowmelt runoff, the dominant flux is in the landward direction. The trapped sediment mass undergoes a repeated cycle of tidal and wind-wave resuspension from shallows and shoals creating a localized turbidity maximum zone. The sediment mass tidally oscillates and contributes to the habitat quality of the Cache Slough Complex. Freshwater pulses episodically flush the Complex. We hypothesize that there is an optimal water and sediment discharge that maximizes net deposition of sediment. We suspect that maximum erosion occurs during Yolo Bypass flows. We intend to test this hypothesis in future work, including analysis of a wet water year when there is flow within the Yolo Bypass floodway, also including Liberty Island flux characteristics and observations of net import/export at LCS.

Acknowledgments We would like to thank those who helped collect this data: Paul Buchanan, Mike Farber, Jessica Wood, Amber Forest, Robert Wilson, and Daniel Whealdon-Haught. We are also grateful for the collaboration with California Department of Water Resources, Sacramento for this work (also providing discharge for UCS) with funding provided by the Interagency Ecological Program. We also appreciate the cooperation of the Solano County Water Agency. We thank Ted Sommer, Neil Ganju, Dr. Johnson U. Kitheka and an anonymous reviewer for their helpful comments on earlier versions of this manuscript.

References

Allen, G.P., J.C. Salomon, P. Bassoullet, Y. Du Penhoat, and C. De Grandpre. 1980. Effects of tides on mixing and suspended sediment transport in macrotidal estuaries. *Sediment Geol* 26: 69–90.

Anderson, C.W. 2004. Turbidity (version 2.0): US Geological Survey Techniques of Water-Resources Investigations, book 9, Chap. A6, section 6.7.

Arthur, J.F. and M.D. Ball. 1979. Factors influencing the entrapment of suspended material in the San Francisco Bay-Delta Estuary. In *San Francisco Bay: the urbanized estuary. Investigations into the natural history of San Francisco Bay and Delta with reference to the influence of man*, ed. T.J. Conomos, 143–174. San Francisco: AAAS

Atwater, B.F., S.G. Conard, J.N. Dowden, C.W. Hedel, R.L. MacDonald, and W. Savage. 1979. History, landforms, and vegetation of the estuary's tidal marshes. In *San Francisco Bay, the urbanized estuary*, ed. T.J. Conomos, 347–385. San Francisco: Pacific Division of the American Association for the Advancement of Science. http://www.estuaryarchive.org/archive/conomos_1979/.

Baskerville-Bridges, B., J.C. Lindberg, and S.I. Doroshov. 2004. The effect of light intensity, alga concentration, and prey density on the feeding behavior of delta smelt larvae. *American Fisheries Society* 39: 219–227.

Brown, L.R. 2003. Will tidal wetland restoration enhance populations of native fishes? San Francisco Estuary and Watershed Science 1 (1): 1–42. http://www.escholarship.org/uc/item/2cp4d8wk.

Brand, A., J.R. Lacy, K. Hsu, D. Hoover, and S. Gladding. 2010. Wind-enhanced resuspension in the shallow water of South San Francisco Bay; mechanisms and potential implications for cohesive sediment transport. *J Geophys Res* 115(C11024): 1–15.

Buchanan, P.A. and T.L. Morgan. 2010 Summary of suspended-sediment concentration data, San Francisco Bay, California, Water Year 2007. US Geological Survey Data Series 476.

Champion, P.D., and C.C. Tanner. 2000. Seasonality of macrophytes and interaction with flow in a New Zealand lowland stream. *Hydrobiologia* 441: 1–12.

Delta Stewardship Council, 2011. Delta Plan: First staff draft. http://www.deltacouncil.ca.gov/docs/draft_delta_plan/Preliminary_Staff_Delta_Plan_2011_02_14.pdf. Accessed March 2011.

Dronkers, J.J. 1986. Tidal asymmetry and estuarine morphology. *Netherlands Journal of Sea Research* 20: 117–131.

Dyer, K.R. 1974. The salt balance in stratified estuaries. *Estuar Coast Mar Sci* 2: 273–281.

Edwards, T.K., and G.D. Glysson. 1999. Field methods for measurement of fluvial sediment. *US Geol. Surv. Tech. Water Resour. Invest* 3: 89. Cahp. C2.

Feyrer, F., K. Newman, M. Nobriga, and T. Sommer. 2011. Modeling the effects of future outflow on the abiotic habitat of an imperiled estuarine fish. *Estuaries and Coasts* 34: 120–128.

Feyrer, F., M.L. Nobriga, and T.R. Sommer. 2007. Multidecadal trends for three declining fish species: habitat patterns and mechanisms in the San Francisco Estuary, California, USA. *Can J Fish Aquat Sci* 64: 723–734.

Friedrichs, C.T., and D.G. Aubrey. 1988. Non-linear tidal distortion in shallow well-mixed estuaries: a synthesis. *Estuaries Coastal and Shelf Science* 27: 521–545.

Ganju, N.K., and D.H. Schoellhamer. 2006. Annual sediment flux estimates in a tidal strait using surrogate measurements. *Estuarine Coastal Shelf Sci* 69: 165–178.

Ganju, N.K., D.H. Schoellhamer, and B.A. Bergamaschi. 2005. Suspended sediment fluxes in a tidal wetland: measurement, controlling factors, and error analysis. *Estuaries* 28(6): 812–822.

Ganju, N.K., D.H. Schoellhamer, J.C. Warner, M.F. Barad, and S.G. Schladow. 2004. Tidal oscillation of sediment between a river and a bay: a conceptual model. *Estuarine Coastal Shelf Sci* 60(1): 81–90.

Geyer, W.R., J.D. Woodruff, and P. Traykovski. 2001. Sedimetn transport and trapping in the Hudson River estuary. *Estuaries* 24: 670–679.

Gilbert, G.K. 1917. Hydraulic mining debris in the Sierra Nevada. US Geological Survey Professional Paper 105.

Grabemann, I., and G. Krause. 1994. Suspended matter fluxes in the turbidity maximum of the Weser Estuary. In *Changes in fluxes in estuaries*, ed. K.R. Dyer and R.J. Orth, 23–28. Denmark: Olsen.

Grabemann, I., R.J. Uncles, G. Krause, and J.A. Stephens. 1997. Behavior of turbidity maxima in the Tamar (U.K.) and Weser (F.R.G.) Estuaries. *Estuarine Coastal Shelf Sci* 45: 234–246.

Gray, J.R., and J.W. Gartner. 2008. Technological advances in suspended-sediment surrogate monitoring. *Water Resour Res* 45: 1–20. W00D29.

Grossinger, R.M., and A. Whipple. 2009. Historical ecology of the California Delta: emerging concepts of a complex and dynamic system. CALFED Science Program Workshop: Ecosystem restoration of the landscape scale. http://www.sfei.org/sites/default/files/ASC_CALFED_DeltaHE_EmergingConcepts_111809.pdf

Guezennec, L., R. Lafite, J.-P. Dupont, and R. Meyer. 1999. Hydrodynamics of suspended particulate matter in the tidal freshwater zone of a macrotidal estuary. *Estuaries* 22(3A): 717–727.

Hamblin, P.F. 1989. Observations and model of sediment transport near the turbidity maximum of the Upper Saint Lawrence Estuary. *J Geophys Res* 94(10): 14,419–14,428.

Helsel, D.R., and R.M. Hirsch. 2002. Statistical methods in water resources-hydrologic analysis and interpretation: US Geological Survey Techniques of Water-Resources Investigations, book 4, Chap. A3. http://pubs.usgs.gov/twri/twri4a3/

James, L.A. 2004. Decreasing sediment yields in Northern California: vestiges of hydraulic gold-mining and reservoir trapping. Sediment transfer through the fluvial system. Proceedings of the Moscow Symposium.

Jassby, A.D., and J.E. Cloern. 2000. Organic matter sources and rehabilitation of the Sacramento–San Joaquin Delta (California, USA). *Aquat Conserv Mar Freshwat Ecosyst* 10: 323–352.

Jassby, A.D., J.E. Cloern, and B.E. Cole. 2002. Annual primary production: patterns and mechanisms of change in a nutrient-rich tidal ecosystem. *Limnol Oceanogr* 47(3): 698–712.

Jay, D.A., and J.D. Musiak. 1994. Particle trapping in estuarine tidal flows. *J Geophys Res* 99(C10): 20,445–20,461.

Jing, L., and P.V. Ridd. 1996. Wave-current bottom shear stresses and sediment resuspension in Cleveland Bay, Australia. *Coast Eng* 29: 169–196.

Kimmerer, W.J. 2002. Physical, biological, and management responses to variable freshwater flow into the San Francisco Estuary. *Estuaries* 25: 1275–1290.

Kitheka, J., G.S. Ongwenyl, and K.M. Mavuti. 2002. Dynamics of suspended sediment exchange and transport in a degraded mangrove creek in Kenya. *Ambio* 31(7/8): 580–587.

Kitheka, J.U., M. Obiero, and P. Nthenge. 2005. River discharge, sediment transport and exchange in the Tana Estuary, Kenya. *Estuarine Coastal Shelf Sci* 63: 455–468.

Kneib, R., C. Simenstad, M. Nobriga, and D. Talley. 2008. Tidal marsh conceptual model. Sacramento–San Joaquin Delta Regional Ecosystem Restoration Implementation Plan.

Krone, R.B. 1979. Sedimentation in the San Francisco Bay System. In *San Francisco Bay: the urbanized estuary*, ed. J.J. Conomos, 85–96. Pacific Division of the American Association for the Advancement of Science, San Francisco.

Lehman, P.W., S. Mayr, L. Mecum, and C. Enright. 2010. The freshwater tidal wetland Liberty Island, CA was both a source and sink of inorganic and organic material to the San Francisco Estuary. *Aquat Ecol* 44(2): 359–372.

Mac Nally, R., J.R. Thomson, W.J. Kimmerer, F. Feyrer, K.B. Newman, A. Sih, W.A. Bennett, L. Brown, E. Fleshman, S.D. Culberson, and G. Castillo. 2010. Analysis of pelagic species decline in the upper San Francisco Estuary using multivariate autoregressive modeling (MAR). *Ecol Appl* 20(5): 1417–1430.

Moyle, P.B., R.A. Daniels, B. Herbold, and D.M. Baltz. 1986. Patterns in distribution and abundance of a noncoevolved assemblage of estuarine fishes in California. *Fish Bull* 84(1): 105–117.

Nobriga, M.L., T.R. Sommer, F. Feyrer, and K. Fleming. 2008. Long-term trends in summertime habitat suitability for delta smelt (*Hypomesus transpacificus*). *San Francisco Estuary and Watershed Science* 6(1): 1–13.

Nobriga, M.L., F. Feyrer, R.D. Baxter, and M. Chotkowski. 2005. Fish community ecology in an altered river delta: spatial patterns in species composition, life history strategies, and biomass. *Estuaries* 5: 776–785.

Rasmussen, P.P., J.R. Gray, G.D. Glysson, and A.C. Ziegler. 2009. Guidelines and procedures for computing time-series suspended-sediment concentrations and loads from in-stream turbidity-sensor and streamflow data. US Geological Survey Techniques and Methods Report 3 C4. http://pubs.usgs.gov/twri/twri3-c4/html/toc.html.

Reed, D.J. 2002. Understanding tidal marsh sedimentation in the Sacramento–San Joaquin Delta, California. *Journal of Coastal Research SI* 36: 605–611.

Roman, M.R., D.V. Holliday, and L.P. Sanford. 2001. Temporal and spatial patterns of zooplankton in the Chesapeake Bay turbidity maximum. *Mar Ecol Prog Ser* 213: 2215–2227.

Ruhl, C.A., and M.R. Simpson. 2005. Computation of discharge using the index velocity method in tidally affected areas. U.S. Geol. Surv. Sci. Invest. Rep. No. 2005-5004, Sacramento.

Sanford, L.P., S.E. Suttles, and J.P. Halka. 2001. Reconsidering the physics of the Chesapeake Bay estuarine turbidity maximum. *Estuaries* 24: 655–669.

Schoellhamer, D.H. 2011. Sudden clearing of estuarine waters upon crossing the threshold from transport to supply regulation of sediment transport as an erodible sediment pool is depleted: San Francisco Bay, 1999. *Estuaries and Coasts* 34: 885–899.

Schoellhamer, D.H. 2001. Influence of salinity, bottom topography, and tides on locations of estuarine turbidity maxima in northern San Francisco Bay. In *Coastal and estuarine fine sediment transport processes,* ed. McAnally, W.H. and Mehta, A.J., 343–357. Amsterdam: Elsevier. http://ca.water.usgs.gov/abstract/sfbay/elsevier0102.pdf

Schoellhamer, D.H. 1996. Factors affecting suspended-solids concentrations in South San Francisco Bay, California. *J Geophys Res* 1010(5): 12087–12095.

Schoellhamer, D.H. 1995. Sediment resuspension mechanisms in Old Tampa Bay, Florida. *Estuarine Coastal Shelf Sci* 40: 603–620.

Schoellhamer, D.H., Wright, S.A., and J.Z. Drexler. 2012. Conceptual Model of Sedimentation in the Sacramento – San Joaquin River Delta. *San Francisco Estuary and Watershed Science* 10(3).

Singer, M.B., R. Aalto, and L.A. James. 2008. Status of the lower Sacramento Valley flood-control system within the context of its natural geomorphic setting. *Natural Hazards Review* 9(3): 104–115.

Sommer, T., F. Mejia, M. Nobriga, F. Feyrer, and L. Grimaldo. 2011. The spawning migration of Delta Smelt in the Upper San Francisco Estuary. *San Francisco Estuary and Watershed Science* 9(2): 1–17.

Sommer, T.S., K. Reece, and F. Mejia. 2009. Delta smelt life-history contingents: A possible upstream rearing strategy? *IEP Newsletter* 22(1): 11–13.

Sommer, T.S., C. Armor, R. Baxter, R. Breuer, L. Brown, M. Chotkowski, S. Culberson, F. Feyrer, M. Gingras, B. Herbold, W. Kimmerer, A. Mueller-Solger, M. Nobriga, and K. Souza. 2007. The collapse of pelagic fishes in the Upper San Francisco Estuary. *Fisheries* 32(6): 270–277.

Sommer, T.R., W.C. Harrel, and T.J. Swift. 2008. Extreme hydrologic banding in a large-river floodplain, California, U.S.A. *Hydrobiologia* 598: 409–415.

Sommerfield, C.K., and K.-C. Wong. 2011. Mechanisms of sediment flux and turbidity maintenance in the Delaware Estuary. *J Geophys Res* 116: C01005. doi:10.1029/2010JC006462.

Son, M., and T.-J. Hsu. 2011. Idealized study on cohesive sediment flux by tidal asymmetry. *Environmental Fluid Mechanics* 11: 183–202.

Tattersall, G.R., A.J. Elliott, and N.M. Lynn. 2003. Suspended sediment concentrations in the Tamar estuary. *Estuarine Coastal Shelf Sci* 57: 679–688.

Uncles, R.J., and J.A. Stephens. 2010. Turbidity and sediment transport in a muddy sub-estuary. *Estuarine Coastal Shelf Sci* 87: 213–224.

Uncles, R.J., and J.A. Stephens. 1993. The freshwater–saltwater interface and its relationship to the turbidity maximum in the Tamar Estuary, UK. *Estuaries* 16: 126–141.

Uncles, R.J., J.A. Stephens, and C. Harris. 2006. Properties of suspended sediment in the estuarine turbidity maximum of the highly turbid Humber-Ouse Estuary, UK. *Ocean Dynamics* 56: 235–247.

Uncles, R.J., R.C.A. Elliot, and S.A. Weston. 1985. Observed fluxes of water, salt and suspended sediment in a partly mixed estuary. *Estuarine Coastal Shelf Sci* 20: 147–167.

USFWS. 2000. Impacts of riprapping to ecosystem functioning, Lower Sacramento River, California. http://www.fws.gov/sacramento/hc/reports/sac_river_riprap.pdf

Wagner, R.J., R.W. Boulger, C.J., Oblinger, and B.A. Smith. 2006. Guidelines and standard procedures for continuous water-quality monitors: station operation, record computation, and data reporting. US Geological Survey Techniques and Methods 1-D3. 51. http://pubs.usgs.gov/tm/2006/tm1D3/

Wall, G.R., E.A. Nystrom, and S. Litten. 2008. Suspended sediment transport in the freshwater reach of the Hudson River Estuary in Eastern New York. *Estuaries and Coasts* 31: 542–553.

Ward, L.G. 1985. The influence of wind waves and tidal currents on sediment resuspension in Middle Chesapeake Bay. *Geo-Mar Lett* 5: 71–75.

Weir, D.J., and J. McManus. 1987. The role of wind in generating a turbidity maximum in the Tay Estuary. *Cont Shelf Res* 7(11/12): 1315–1318.

Whipple, A. 2010. Historical ecology of the Delta: Habitat characteristics of a fluvial-tidal landscape. 2010 Interagency Ecological Program Workshop. http://www.sfei.org/sites/default/files/ASC_HIstoricalEcologyNorthDelta_IEP_052610.pdf

Wilcox, R.J., P.D. Champion, J.W. Nagels, and G.F. Croker. 1999. The influence of aquatic macrophytes on the hydraulic and physico-chemical properties of a New Zealand lowland stream. *Hydrobiologia* 416: 203–214.

Wolanski, E., B. King, and D. Galloway. 1995. Dynamics of the turbidity maximum in the Fly River Estuary, Papua New Guinea. *Estuarine Coastal Shelf Sci* 40: 321–337.

Wright, S.A., and D.H. Schoellhamer. 2005. Estimating sediment budgets at the interface between river and estuaries with application to the Sacramento-San Joaquin River Delta. *Water Resour Res* 41(W09428): 1–17.

Wright, S.A., and D.H. Schoellhamer. 2004. Trends in the sediment yield of the Sacramento River, California, 1957–2001. *San Francisco Estuary and Watershed Science, 2*(2), 2. http://repositories.cdlib.org/jmie/sfews/vol2/iss2/art2